

Preparation and X-ray Structures of Platinum and Palladium Complexes of the Chalcogen-Substituted Diazenes *trans*-[PhEN(4-CH₃C₆H₄)CN=NC(4-CH₃C₆H₄)NEPh] (E = S, Se)

Tristram Chivers,* Katherine McGregor, and Masood Parvez

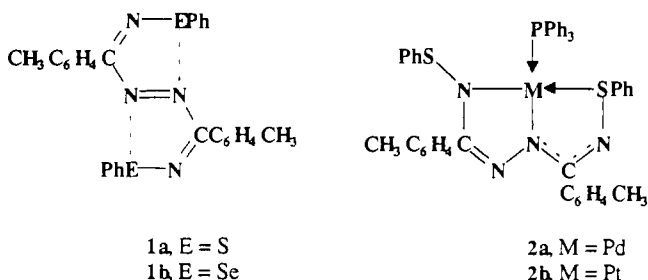
Department of Chemistry, The University of Calgary, 2500 University Drive N.W. Calgary, Alberta T2N 1N4, Canada

Received November 24, 1993*

The reaction of the chalcogen-substituted diazenes *trans*-[PhEN(4-CH₃C₆H₄)CN=NC(4-CH₃C₆H₄)NEPh] (E = S, Se) with Pd(PPh₃)₄ or Pt(C₂H₄)(PPh₃)₂ in toluene produces the complexes M[PhEN(4-CH₃C₆H₄)CN=NC(4-CH₃C₆H₄)NEPh](PPh₃) (2a, M = Pd, E = S; 2b, M = Pt, E = S; 2c, M = Pd, E = Se; 2d, M = Pt, E = Se). The ¹H NMR spectra of 2a–d show two singlets at 2.26–2.29 and 2.35–2.39 ppm for the 4-CH₃ protons, and the ⁷⁷Se NMR spectrum of 2c exhibits two equally intense singlets at 872 and 882 ppm. The ³¹P{¹H} NMR spectra exhibit a singlet at 25–26 ppm for 2a and 2c and at 19–20 ppm [¹J(³¹P–¹⁹⁵Pt) = 3610–3630 Hz] for 2b and 2d. X-ray structural determinations have revealed that the coordination sites of the approximately square planar metal complexes 2a–d are occupied by a single PPh₃ molecule and a tridentate (N, N, E) ligand. The N–N bond distances in these complexes are 1.40–1.42 Å, indicating formal reduction of the diazene to an azine. Crystals of 2c are monoclinic, P2₁/c, with a = 14.354(1) Å, b = 19.007(3) Å, c = 16.157(2) Å, β = 104.92(1)°, V = 4259(1) Å³, Z = 4, R = 0.040, and R_w = 0.024. Crystals of 2d are monoclinic, P2₁/c, with a = 14.410(3) Å, b = 19.003(3) Å, c = 16.169(2) Å, β = 105.72(1)°, V = 4261(1) Å³, Z = 4, R = 0.040, R_w = 0.025. The FAB mass spectra for the sulfur complexes 2a and 2b show a strong molecular ion peak whereas this peak either is absent (2c) or is of low intensity (2d) for the selenium complexes. The complexes 2a and 2b undergo reversible one-electron oxidations at ca. 0.65 V vs SCE, but the oxidation product has a lifetime of only a few seconds.

Introduction

In recent years there has been considerable interest concerning the coordination chemistry of chalcogen–nitrogen ligands with the platinum group metals. Much of this work has focused on complexes of S–N ligands,^{1,2} while the coordination chemistry of the corresponding Se–N systems is less well-developed. In general, this may be attributed to the greater instability of the Se–N linkage. Chalcogen-substituted diazenes of the type 1³ are expected to be versatile polydentate ligands in view of the number and variety of heteroatoms available for coordination. In a preliminary communication, we reported that the reaction of the sulfur-substituted diazene 1a with zerovalent platinum or palladium complexes unexpectedly produces the formally divalent tridentate (N, N, S) azine metallacycles 2.⁴



We have now carried out the corresponding reactions of the selenium analogue 1b and we describe here the full details of our investigations of the reactions of both 1a and 1b with zerovalent

group 10 metals. This includes (a) the preparation, spectroscopic and X-ray structural characterization of the four metallacycles M[PhEN(4-CH₃C₆H₄)CN=NC(4-CH₃C₆H₄)NEPh]PPh₃ (M = Pt, Pd; E = S, Se) and (b) FAB MS and electrochemical studies of these complexes.

Experimental Section

Reagents and General Procedures. All reactions and manipulations were performed under an atmosphere of dry argon gas using standard Schlenk techniques. All solvents were dried and distilled before use: toluene, THF, hexanes, diethyl ether (sodium benzophenone), CH₂Cl₂ (P₂O₅), and acetonitrile (CaH₂, P₂O₅, CaH₂). The compounds *trans*-PhSN(4-CH₃C₆H₄)CN=NC(4-CH₃C₆H₄)NSPh,^{3a} (4-CH₃C₆H₄)CN₂(SiMe₃)₃,⁵ and (C₂H₄)Pt(PPh₃)₂⁶ were prepared according to the published procedure. Pd(PPh₃)₄ and PhSeCl (Aldrich) were used as received. The elemental analyses were performed by the microanalytical service within the Chemistry Department at The University of Calgary.

Instrumentation. ³¹P{¹H} and ⁷⁷Se{¹H}NMR spectra were recorded for THF solutions on a Bruker AM-400 spectrometer operating at 161.978 and 76.312 MHz, respectively. A D₂O insert was used as the lock. Routine proton NMR spectra were run on a Bruker AC-200 at 200.132 MHz. The solvent deuterium resonance served as the lock. ³¹P NMR chemical shifts are reported in ppm relative to 85% H₃PO₄, and ⁷⁷Se NMR chemical shifts are reported relative to Me₂Se. Electrochemical measurements were performed by using a Hi-Tek DT2101 potentiostat operating in conjunction with a Hi-Tek PPR1 waveform generator. The FAB mass spectra were recorded on a Kratos MS80 RFA spectrometer by using a Phrasor Scientific Cs ion gun and nitrobenzyl alcohol/CH₂Cl₂ matrices.

Preparation of *trans*-[PhSeN(4-CH₃C₆H₄)CN=NC(4-CH₃C₆H₄)NSePh] (1b). A solution of PhSeCl (2.4 g, 12.5 mmol) in CH₂Cl₂ (20 mL) was added dropwise to a solution of 4-CH₃C₆H₄CN₂(SiMe₃)₃ (1.47 g, 4.18 mmol) in CH₂Cl₂ (20 mL) at –78 °C. The reaction was allowed to attain ambient temperature and stirred for 3 h. After such time the solvent was removed under reduced pressure and the residue was extracted with hexanes (2 × 40 mL) to remove Ph₂Se₂ formed as a byproduct. The

* Abstract published in *Advance ACS Abstracts*, April 15, 1994.

- (1) Chivers, T.; Edelmann, F. *Polyhedron* **1986**, *5*, 1661.
- (2) Kelly, P. F.; Woollins, J. D. *Polyhedron* **1986**, *5*, 607.
- (3) (a) Chandrasekhar, V.; Chivers, T.; Kumaravel, S. S.; Parvez, M.; Rao, M. N. S.; *Inorg. Chem.* **1991**, *30*, 4125. (b) Chandrasekhar, V.; Chivers, T.; Fait, J. F.; Kumaravel, S. S. *J. Am. Chem. Soc.* **1990**, *112*, 5374.
- (4) Chivers, T.; McGregor, K.; Parvez, M. *J. Chem. Soc., Chem. Commun.* **1993**, 1021.

(5) Boeré, R. T.; Oakley, R. T.; Reed, R. W. *J. Organomet. Chem.* **1987**, *331*, 161.

(6) Nagel, U. *Chem. Ber.* **1982**, *115*, 1998.

Table 1. Crystallographic Data for Pd(PhSeN(4-CH₃C₆H₄)CN-NC(4-CH₃C₆H₄)NSePh)(PPh₃)·0.5THF and Pt(PhSeN(4-CH₃C₆H₄)CN-NC(4-CH₃C₆H₄)NSePh)(PPh₃)·0.5Et₂O

formula	C ₄₈ H ₄₄ N ₄ O _{0.5} PSe ₂ Pt	C ₄₈ H ₄₄ N ₄ O _{0.5} PSe ₂ Pd
fw	1068.89	979.19
space group	P2 ₁ /c (No. 14)	P2 ₁ /c (No. 14)
a, Å	14.410(1)	14.354(3)
b, Å	19.003(3)	19.007(3)
c, Å	16.169(2)	16.157(2)
β, deg	105.72(1)	104.92(1)
V, Å ³	4261(1)	4259(1)
Z	4	4
T, °C	23	23
λ, Å	0.710 69	0.710 69
ρ _{calcd} , g cm ⁻³	1.666	1.527
μ, mm ⁻¹	5.065	2.223
R ^a	0.040	0.040
R _w ^b	0.025	0.024

$$^a R = \sum |F_o| - |F_c| / \sum |F_o|, \quad ^b R_w = [\sum w\Delta^2 / \sum wF_o^2]^{1/2}.$$

hexanes-insoluble purple solid was recrystallized from a 1:3 mixture of CH₂Cl₂/hexanes at -18 °C, producing **1b** as a purple/brown solid in 80% yield. Anal. Calcd for C₂₈H₂₄N₄Se₂: C, 58.55; H, 4.21; N, 9.75. Found: C, 58.84; H, 4.20; N, 10.12. ¹H NMR (CDCl₃): 2.49 (s, 4-CH₃C₆H₄, 3H), 7.29–7.65 (m, C₆H₅, 5H), 8.09 ppm (dd, CH₃C₆H₄, 4H). ⁷⁷Se{¹H} NMR (THF) 995 ppm (s).

Pd(PhSN(4-CH₃C₆H₄)CN-NC(4-CH₃C₆H₄)NSPh)(PPh₃) (2a). A toluene solution (20 mL) of **1a** (0.05 g, 10.4 mmol) was added dropwise to a toluene solution (15 mL) of Pd(PPh₃)₄ (0.12 g, 10.4 mmol) at -78 °C over a period of ca. 30 min. Several aliquots of toluene (3 × 10 mL) were used to wash residual **1a** into the reaction vessel. On warming the solution to ambient temperature, the characteristic vivid purple color of **1a** remained. After stirring at room temperature overnight, the solution became red. The solvent was removed under reduced pressure and the red residue was recrystallized from a 1:2 mixture of THF/hexanes at room temperature, producing X-ray quality crystals of **2a** in 85% yield. Anal. Calcd for C₄₆H₃₉N₄PPdS₂: C, 65.05; H, 4.63; N, 6.60. Found: C, 64.68; H, 4.93; N, 6.20. ³¹P NMR (THF): 25.69 ppm (s), ¹H NMR (CDCl₃): 8.00–6.47 (m, C₆H₅ and CH₃C₆H₄, 33H), 2.36 (s, CH₃C₆H₄, 3H), 2.26 ppm (s, CH₃C₆H₄, 3H).

Pt(PhSN(4-CH₃C₆H₄)CN-NC(4-CH₃C₆H₄)NSPh)(PPh₃) (2b). A toluene solution (20 mL) of **1a** (0.05 g, 10.4 mmol) was added dropwise to a toluene solution (15 mL) of (C₂H₄)Pt(PPh₃)₂ (0.075 g, 10.4 mmol) at -78 °C over a period of ca. 30 min. Several aliquots of toluene (3 × 10 mL) were used to wash residual **1a** into the reaction vessel. When the solution was warmed to ambient temperature, the characteristic vivid purple color of **1a** gradually disappeared. After ca. 30 min of stirring at room temperature, the solution became bright yellow. The solvent volume was reduced to ca. 10–15 mL and stored for several hours at -18 °C. After such time a bright yellow precipitate was isolated and washed with hexanes (2 × 10 mL). X-ray quality crystals of **2b** were grown from a 1:2 mixture of THF/hexanes at ambient temperature in 65% yield. Anal. Calcd for C₄₆H₃₉N₄PPtS₂·0.5C₄H₈O: C, 58.90; H, 4.19; N, 5.97. Found: C, 58.86; H, 4.36; N, 5.73. ³¹P NMR (THF): 19.51 ppm (s), ¹J(¹⁹⁵Pt–³¹P) = 3612 Hz. ¹H NMR (CDCl₃): 8.04–6.39 (m, C₆H₅ and CH₃C₆H₄, 33H), 2.35 (s, CH₃C₆H₄, 3H), 2.27 ppm (s, CH₃C₆H₄, 3H).

Pd(PhSeN(4-CH₃C₆H₄)CN-NC(4-CH₃C₆H₄)NSePh)(PPh₃) (2c). This was prepared using an analogous procedure to that described for the preparation of **2a**. Yield: 62%. X-ray quality crystals of **2c** were grown from a 1:2 mixture of THF/ether at ambient temperature. Anal. Calcd for C₄₆H₃₉N₄PPdSe₂: C, 58.58; H, 4.17; N, 5.94. Found: C, 58.18; H, 4.12; N, 5.46. ³¹P NMR (THF): 25.28 ppm (s). ⁷⁷Se NMR (THF): 882 (s), 778 ppm (s). ¹H NMR (CDCl₃): 7.86–6.67 (m, C₆H₅ and CH₃C₆H₄, 33H), 2.35 (s, CH₃C₆H₄, 3H), 2.26 (s, CH₃C₆H₄, 3H).

Pt(PhSeN(4-CH₃C₆H₄)CN-NC(4-CH₃C₆H₄)NSePh)(PPh₃) (2d). This was prepared using an analogous procedure to that described for the preparation of **2b**. Required ca. 30 min of stirring at ambient temperature for the reaction to proceed to completion. Yield: 40%. X-ray quality crystals of **2d** were grown from a 1:2 mixture of CH₂Cl₂/ether at ambient temperature. Anal. Calcd for C₄₆H₃₉N₄PPtSe₂: C, 53.55; H, 3.81; N, 5.43. Found: C, 54.03; H, 4.16; N, 5.01. ³¹P NMR (THF): 19.14 ppm (s), ¹J(¹⁹⁵Pt–³¹P) = 3627 Hz. ¹H NMR (CD₂Cl₂): 6.59–7.77 (m, C₆H₅ and CH₃C₆H₄, 33H), 2.39 (s, CH₃C₆H₄, 3H), 2.29 ppm (s, CH₃C₆H₄, 3H).

X-ray Analyses. 2c. A suitable colorless crystal of Pd(PhSeN(4-CH₃C₆H₄)CN-NC(4-CH₃C₆H₄)NSePh)(PPh₃)·0.5THF was obtained

Table 2. Final Fractional Coordinates and Equivalent Isotropic Temperature Factors B_{eq} (Å²) with Esd's in Parentheses for Pd(PhSeN(4-CH₃C₆H₄)CN-NC(4-CH₃C₆H₄)NSePh)(PPh₃)·0.5THF

atom	x	y	z	B _{eq} ^a
Pd(1)	0.20052(5)	0.02511(3)	-0.13195(4)	2.79(2)
Se(1)	0.27956(6)	0.13431(5)	-0.13634(5)	3.02(2)
Se(2)	0.10556(7)	-0.14288(5)	-0.13832(6)	3.75(3)
P(1)	0.1425(2)	0.0073(1)	-0.2770(1)	3.39(6)
N(1)	0.1391(4)	-0.0575(3)	-0.0872(4)	3.0(2)
N(2)	0.2017(5)	-0.0024(3)	0.0455(4)	2.7(2)
N(3)	0.2391(4)	0.0444(3)	-0.0059(3)	2.5(2)
N(4)	0.3146(4)	0.1521(3)	-0.0186(4)	3.1(2)
C(1)	0.2241(7)	-0.1937(5)	-0.1079(5)	3.6(3)
C(2)	0.3106(7)	-0.1643(5)	-0.0603(5)	4.4(3)
C(3)	0.3955(7)	-0.2023(6)	-0.0454(6)	5.2(3)
C(4)	0.3979(8)	-0.2695(6)	-0.0746(7)	6.2(4)
C(5)	0.3121(9)	-0.2993(5)	-0.1207(7)	5.6(4)
C(6)	0.2265(7)	-0.2624(5)	-0.1375(5)	4.5(3)
C(7)	0.1554(6)	-0.0539(4)	0.0016(5)	2.7(2)
C(8)	0.1093(6)	-0.1064(4)	0.0471(5)	2.6(2)
C(9)	0.1605(6)	-0.1586(5)	0.0978(5)	3.7(3)
C(10)	0.1142(7)	-0.2078(4)	0.1355(5)	4.0(3)
C(11)	0.0155(6)	-0.2065(4)	0.1242(5)	3.0(2)
C(12)	-0.0351(6)	-0.1541(4)	0.0734(5)	3.5(2)
C(13)	0.0107(6)	-0.1051(4)	0.0348(5)	3.1(2)
C(14)	-0.0347(6)	-0.2598(5)	0.1662(6)	5.4(3)
C(15)	0.2823(6)	0.1040(4)	0.0265(5)	2.7(2)
C(16)	0.2992(6)	0.1212(4)	0.1203(5)	3.0(2)
C(17)	0.3909(6)	0.1370(5)	0.1687(5)	4.3(3)
C(18)	0.4049(6)	0.1542(5)	0.2543(5)	4.4(3)
C(19)	0.3302(7)	0.1595(5)	0.2914(5)	4.1(3)
C(20)	0.2393(7)	0.1464(5)	0.2424(6)	4.5(3)
C(21)	0.2234(6)	0.1270(4)	0.1571(5)	3.7(2)
C(22)	0.3484(7)	0.1777(4)	0.3865(5)	6.0(3)
C(23)	0.4043(6)	0.1114(4)	-0.1510(5)	3.2(2)
C(24)	0.4561(8)	0.0565(5)	-0.1110(6)	5.3(3)
C(25)	0.5470(9)	0.0416(6)	-0.1224(8)	7.2(4)
C(26)	0.5846(9)	0.0820(8)	-0.1733(8)	7.8(5)
C(27)	0.5351(8)	0.1389(7)	-0.2129(7)	7.0(4)
C(28)	0.4442(7)	0.1544(5)	-0.2018(6)	4.6(3)
C(29)	0.1996(6)	-0.0621(5)	-0.3235(5)	3.6(3)
C(30)	0.2706(7)	-0.1009(5)	-0.2701(6)	4.4(3)
C(31)	0.3173(8)	-0.1544(6)	-0.3022(7)	6.3(4)
C(32)	0.2953(9)	-0.1672(6)	-0.3880(9)	7.1(5)
C(33)	0.2267(9)	-0.1277(6)	-0.4431(7)	7.2(4)
C(34)	0.1791(7)	-0.0750(5)	-0.4115(6)	5.2(3)
C(35)	0.0128(6)	-0.0062(4)	-0.3037(5)	3.5(2)
C(36)	-0.0387(7)	0.0224(5)	-0.2512(6)	4.9(3)
C(37)	-0.1374(8)	0.0220(6)	-0.2715(6)	6.3(3)
C(38)	-0.1866(7)	-0.0074(6)	-0.3465(7)	5.9(4)
C(39)	-0.1392(8)	-0.0387(6)	-0.3985(6)	5.6(3)
C(40)	-0.0398(7)	-0.0376(5)	-0.3790(6)	5.1(3)
C(41)	0.1547(8)	0.0847(5)	-0.3416(5)	3.9(3)
C(42)	0.0809(8)	0.1309(6)	-0.3726(7)	6.5(4)
C(43)	0.096(1)	0.1910(6)	-0.4168(7)	7.9(4)
C(44)	0.183(1)	0.2029(6)	-0.4315(8)	7.7(5)
C(45)	0.2581(9)	0.1572(6)	-0.4017(7)	6.9(4)
C(46)	0.2425(8)	0.0972(5)	-0.3571(6)	5.2(3)
O(1)	0.550(5)	0.040(4)	0.564(7)	21(2)
C(47)	0.559(4)	0.024(4)	0.477(6)	21(1)
C(48)	0.499(6)	0.008(2)	0.574(5)	30(2)

$$^a B_{eq} = \frac{1}{3} \pi^2 (U_{11}(aa^*)^2 + U_{22}(bb^*)^2 + U_{33}(cc^*)^2 + 2U_{12}aa^*bb^* \cos \gamma + 2U_{13}aa^*cc^* \cos \beta + 2U_{23}bb^*cc^* \cos \alpha).$$

by recrystallization from THF/Et₂O at ambient temperature. Accurate cell dimensions and a crystal orientation matrix were determined on a Rigaku AFC6S diffractometer by a least-squares fit of the setting angles of 25 reflections with 2θ in the range 27–35°. Intensity data were collected by the ω/2θ method using a scan speed of 4.0°/min, scan width of (1.10 + 0.34 tan θ)° and monochromatized Mo Kα radiation in the range 4 < 2θ < 50° with h = 0 to 16, k = 0 to 22, and l = -18 to +18. Three reflections were monitored every 2 h of exposure time and showed insignificant variations. The intensities of 7796 reflections were measured, of which 3382 had I > 3σ(I). Data were corrected for Lorentz, polarization and absorption effects,⁷ the correction range being 0.9026–0.9998. Crystal data are summarized in Table 1, and the positional parameters are given in Table 2.

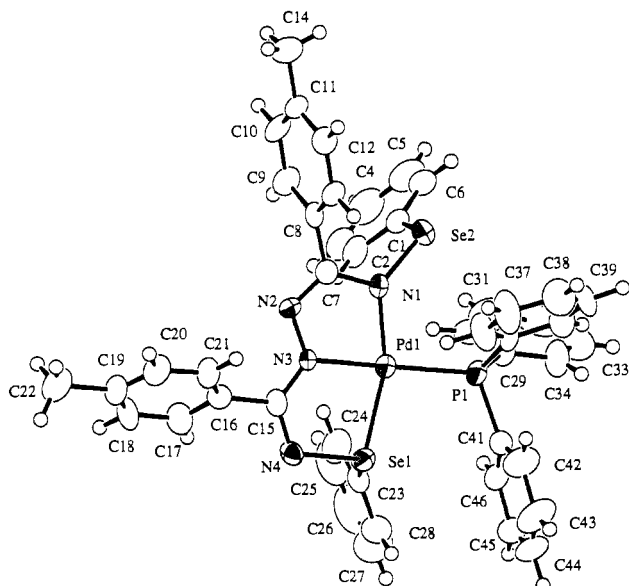


Figure 1. ORTEP plot for Pd(PhSeN(4-CH₃C₆H₄)CN-NC(4-CH₃C₆H₄)NSePh)(PPh₃)·0.5THF (**2c**) with the THF molecule omitted.

The structure was solved by the Patterson method⁸ and expanded using Fourier techniques.⁹ Refinement of the structure was by full-matrix least-squares calculations, initially with isotropic and finally with anisotropic temperature factors for the non-hydrogen atoms. Hydrogen atoms were included at geometrically idealized positions and were not refined. The THF solvate shows large thermal vibrations reflecting disorder. Refinement converged with $R = 0.040$ and $R_w = 0.020$. In the refinement cycles, weights were derived from the counting statistics. Scattering factors were those of Cromer and Waber¹⁰ and Stewart, Davidson, and Simpson¹¹ and allowance was made for anomalous dispersion.¹² A difference map calculated at the conclusion of the refinement had no chemically significant features. The computer programs used were part of TEXSAN¹³ installed on a Silicon Graphics Personal Iris 4D/35 computer. Figure 1 was plotted using ORTEP II.¹⁴

2d. A suitable colorless crystal of Pt(PhSeN(4-CH₃C₆H₄)CN-NC(4-CH₃C₆H₄)NSePh)(PPh₃)·0.5Et₂O was obtained by recrystallization from CH₂Cl₂/Et₂O at ambient temperature. Accurate cell dimensions and a crystal orientation matrix were determined on a Rigaku AFC6S diffractometer by a least-squares fit of the setting angles of 25 reflections with 2θ in the range 18–31°. Intensity data were collected by the $\omega/2\theta$ method using a scan speed of 2.0°/min, scan width of $(0.89 + 0.34 \tan \theta)^\circ$, and monochromatized Mo K α radiation in the range $4 < 2\theta < 50^\circ$ with $h = 0$ to 16, $k = 0$ to 22, and $l = -19$ to +19. Three reflections were monitored every 2 h of exposure time and showed insignificant variations. The intensities of 7808 reflections were measured, of which 2900 had $I > 3\sigma(I)$. Data were corrected for Lorentz, polarization, and absorption effects,⁷ the correction range being 0.8018–0.9995. Crystal data are summarized in Table 1, while the positional parameters are given in Table 3.

The structure was solved in an analogous manner to that of **2d**. The diethyl ether solvate shows large thermal vibrations reflecting disorder.

Table 3. Final Fractional Coordinates and Equivalent Isotropic Temperature Factors B_{eq} (Å²) with Esd's in Parentheses for Pt(PhSeN(4-CH₃C₆H₄)CN-NC(4-CH₃C₆H₄)NSePh)(PPh₃)·0.5Et₂O

atom	x	y	z	B_{eq}
Pt(1)	0.19772(4)	0.02491(3)	0.86777(4)	2.88(2)
Se(1)	0.27710(11)	0.13335(7)	0.86331(9)	3.21(7)
Se(2)	0.10352(11)	-0.14298(8)	0.86087(9)	4.05(8)
P(1)	0.1378(3)	0.0073(2)	0.7242(2)	3.5(2)
N(1)	0.1382(7)	-0.0576(5)	0.9127(6)	3.1(5)
N(2)	0.2026(7)	-0.0033(5)	1.0453(6)	2.8(6)
N(3)	0.2361(7)	0.0443(5)	0.9930(6)	2.6(5)
N(4)	0.3133(8)	0.1524(6)	0.9824(6)	3.5(6)
C(1)	0.2222(11)	-0.1943(8)	0.8922(9)	4.3(8)
C(2)	0.3097(12)	-0.1636(8)	0.9403(9)	4.5(8)
C(3)	0.3930(13)	-0.2035(10)	0.9558(10)	5.8(10)
C(4)	0.3955(13)	-0.2701(10)	0.9249(11)	6.1(10)
C(5)	0.3086(15)	-0.3013(9)	0.8772(11)	6.0(9)
C(6)	0.2230(13)	-0.2623(9)	0.8625(10)	5.4(9)
C(7)	0.1547(10)	-0.0524(7)	1.0021(8)	3.1(7)
C(8)	0.1070(10)	-0.1062(7)	1.0463(7)	2.7(7)
C(9)	0.1601(10)	-0.1595(8)	1.0969(9)	3.6(7)
C(10)	0.1135(11)	-0.2088(7)	1.1340(8)	3.6(7)
C(11)	0.0152(10)	-0.2061(7)	1.1238(9)	3.4(7)
C(12)	-0.0340(9)	-0.1540(7)	1.0719(9)	3.2(7)
C(13)	0.0114(9)	-0.1059(7)	1.0351(8)	3.3(7)
C(14)	-0.0336(11)	-0.2598(8)	1.1671(9)	5.5(8)
C(15)	0.2818(10)	0.1038(7)	1.0271(8)	3.0(7)
C(16)	0.3000(12)	0.1226(7)	1.1190(9)	3.5(7)
C(17)	0.3900(11)	0.1385(8)	1.1685(10)	4.4(8)
C(18)	0.4083(10)	0.1569(8)	1.2534(9)	4.6(8)
C(19)	0.3333(12)	0.1593(7)	1.2917(9)	3.8(7)
C(20)	0.2415(11)	0.1455(7)	1.2415(9)	4.3(8)
C(21)	0.2235(10)	0.1250(7)	1.1578(8)	3.6(7)
C(22)	0.3533(12)	0.1773(7)	1.3871(9)	5.4(9)
C(23)	0.4023(10)	0.1102(8)	0.8516(8)	3.3(7)
C(24)	0.4540(12)	0.0540(8)	0.8913(10)	4.9(9)
C(25)	0.5436(14)	0.0387(10)	0.8810(11)	6.8(10)
C(26)	0.5839(13)	0.0836(12)	0.8320(13)	6.7(9)
C(27)	0.5359(14)	0.1415(10)	0.7963(11)	6.3(9)
C(28)	0.4461(11)	0.1530(8)	0.8048(10)	4.9(9)
C(29)	0.1960(10)	-0.0591(7)	0.6758(8)	3.3(7)
C(30)	0.2658(11)	-0.1020(8)	0.7279(9)	4.4(8)
C(31)	0.3123(12)	-0.1519(9)	0.6945(12)	5.6(10)
C(32)	0.2892(15)	-0.1649(9)	0.6089(13)	6.6(10)
C(33)	0.2224(14)	-0.1228(10)	0.5541(11)	6.6(9)
C(34)	0.1749(12)	-0.0725(9)	0.5878(9)	5.5(9)
C(35)	0.0085(10)	-0.0081(6)	0.6961(8)	3.6(7)
C(36)	-0.0463(12)	0.0236(9)	0.7458(9)	5.2(8)
C(37)	-0.1438(11)	0.0198(9)	0.7236(10)	5.9(9)
C(38)	-0.1903(13)	-0.0109(9)	0.6482(12)	6.4(10)
C(39)	-0.1416(13)	-0.0429(10)	0.5972(10)	6.3(9)
C(40)	-0.0441(12)	-0.0409(8)	0.6217(8)	4.6(8)
C(41)	0.1481(12)	0.0854(8)	0.6606(9)	3.7(7)
C(42)	0.2339(13)	0.1011(8)	0.6475(10)	5.0(10)
C(43)	0.2477(15)	0.1613(12)	0.6021(11)	7.5(10)
C(44)	0.1725(18)	0.2038(10)	0.5691(12)	6.8(9)
C(45)	0.0850(16)	0.1905(11)	0.5827(13)	8.4(9)
C(46)	0.0719(13)	0.1301(9)	0.6269(10)	5.9(9)
O(1)	0.476(4)	-0.012(2)	0.463(4)	17.7(8)
C(47)	0.542(3)	0.007(2)	0.457(4)	26.6(7)
C(48)	0.536(2)	-0.006(2)	0.381(2)	16.7(9)

$${}^a B_{eq} = \frac{8}{3}\pi^2(U_{11}(aa^*)^2 + U_{22}(bb^*)^2 + U_{33}(cc^*)^2 + 2U_{12}aa^*bb^* \cos \gamma + 2U_{13}aa^*cc^* \cos \beta + 2U_{23}bb^*cc^* \cos \alpha)$$

Refinement converged with $R = 0.040$ and $R_w = 0.025$. Figure 2 was plotted using ORTEP II.¹⁴

Results and Discussion

Synthesis of *trans*-[PhSeN(4-CH₃C₆H₄)CN=NC(4-CH₃C₆H₄)NSePh] (1b**).** In order to have a convenient ¹H NMR probe for the structures of metal complexes, we chose to work with the *C-p*-tolyl derivatives of the chalcogen-substituted azo dyes **1a** and **1b** rather than the *C-phenyl* compound. The preparation and spectroscopic characterization of the new selenium derivative **1b** is described here. The reaction of 4-CH₃C₆H₄CN₂(SiMe₃)₃ with 3 molar equiv of PhSeCl in CH₂Cl₂ at -78 °C produces an

- (7) North, A. C. T.; Phillips, D. C.; Mathews, F. S. *Acta Crystallogr.* **1968**, *A24*, 351.
- (8) PATTY: Beurskens, P. T.; Admiraal, G.; Beurskens, G.; Bosman, W. P.; Garcia-Granda, S.; Gould, R. O.; Smits, J. M. M.; Smykalla, C. The DIRDIF program system. Technical report of the Crystallography Laboratory, University of Nijmegen, The Netherlands, 1992.
- (9) DIRDIF92: Beurskens, P. T.; Admiraal, G.; Beurskens, G.; Bosman, W. P.; Garcia-Granda, S.; Gould, R. O.; Smits, J. M. M.; Smykalla, C. The DIRDIF program system. Technical report of the Crystallography Laboratory, University of Nijmegen, The Netherlands, 1992.
- (10) Cromer, D. T.; Waber, J. T. *International Tables for Crystallography*, **1974**, Vol. IV, Kynoch Press: Birmingham, England, 1974; Vol. IV, Table 2.2A, pp 71–98.
- (11) Stewart, R. F.; Davidson, E. R.; Simpson, W. T. *J. Chem. Phys.* **1965**, *42*, 3175.
- (12) Cromer, D. T.; Liberman, D. *J. Chem. Phys.* **1970**, *53*, 1891.
- (13) TEXSAN. Single Crystal Structure Analysis Software, Version 1.2. Molecular Structure Corporation, The Woodlands, TX, 1992.
- (14) Johnson, C. K. *ORTEP II*; Report ORNL-5138; Oak Ridge National Laboratory: Oak Ridge, TN, 1976.

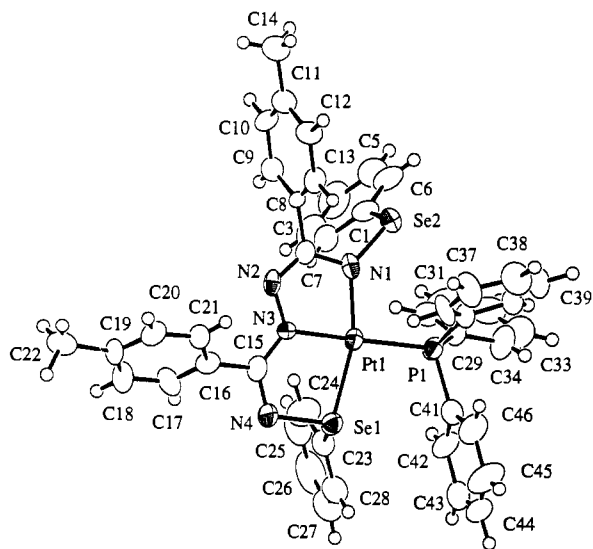
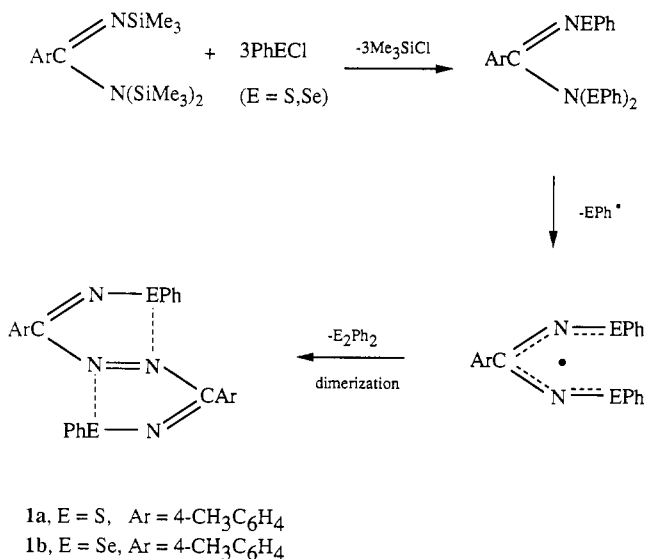


Figure 2. ORTEP plot for Pt(PhSeN(4-CH₃C₆H₄)CN-NC(4-CH₃C₆H₄)NSePh)(PPh₃)·0.5Et₂O (**2d**) with the Et₂O molecule omitted.

Scheme 1. Proposed Mechanism for the Formation of the Diazenes **1a** and **1b**



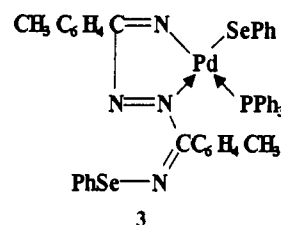
intensely colored purple solution upon warming to room temperature. The purple diazene **1b** was isolated as the final product in 80% yield and has been characterized by microanalysis, ¹H and ⁷⁷Se{¹H} NMR spectroscopy. Diphenyl diselenide was obtained as a byproduct in almost quantitative yield as required by the reaction pathway outlined in Scheme 1. ESR studies of analogous systems have provided evidence for the radical pathway described in Scheme 1.^{3a}

The ¹H NMR spectrum of **1b** in CDCl₃ solution shows a singlet at 2.49 ppm, a multiplet at 7.29 to 7.65 ppm, and a doublet of doublets at 8.09 ppm, which is consistent with the proposed formulation. The ⁷⁷Se{¹H} NMR spectrum of a THF solution of **1b** shows a single resonance at 995 ppm. An important feature of the spectroscopic data for **1b** is the clear indication of equivalent 4-CH₃C₆H₄ and SePh groups within the diazene ligand. The properties of **1b** suggest that the solid-state structure resembles that of the structurally characterized diazene *trans*-[MeSeN(Ph)CN=NC(Ph)NSeMe] (**1c**);^{3b} i.e. **1b**, also contains intramolecular interactions between each of the selenium atoms and one of the nitrogen atoms of the azo group.

Reaction of 1b with Pd(PPh₃)₄. The reaction of **1a** or **1b** with an equimolar amount of Pd(PPh₃)₄ in toluene at ambient temperature produces **2a** and **2c** in 85% and 62% yields,

respectively. Compounds **2a** and **2c** are both obtained as air-stable red crystals. The ³¹P{¹H} NMR spectra of **2a** and **2c** in THF solution exhibit a singlet at 25–26 ppm (cf. Pd(PPh₃)₄, δ(³¹P) 18.4 ppm¹⁵), while the ¹H NMR spectra exhibit two singlets at 2.35 and 2.26 ppm, in addition to a number of complex multiplets in the aromatic region. Two signals of similar intensity were also observed in the ⁷⁷Se{¹H} NMR spectrum of **2c**, at 882 and 778 ppm respectively. Coupling between ³¹P and ⁷⁷Se nuclei is not observed. These results indicate the presence of inequivalent 4-CH₃C₆H₄ and SePh groups in these complexes and a single environment for phosphorus.

The similarity of the spectroscopic data obtained for **2a** and **2c** suggest that the sulfur and selenium complexes with palladium may be isostructural. However, there is another possible formulation for **2c** which cannot be discounted on the basis of microanalytical and spectroscopic evidence alone. A common reaction of chalcogen–nitrogen ligands is the insertion of a metal fragment into the chalcogen–nitrogen bond^{1,2,16,17} which, in the present case, would give the complex **3**.



In this type of complex, the N=N double bond in the diazene is retained and the ligand adopts a bidentate mode of coordination. In order to distinguish between these structural possibilities for **2c** an X-ray crystallographic determination was performed.

Crystal and Molecular Structure of 2c. An X-ray structural study identified **2c** as the azine metallacycle Pd(PhSeN(4-CH₃C₆H₄)CN-NC(4-CH₃C₆H₄)NSePh)(PPh₃)·0.5THF. Figure 1 is an ORTEP diagram showing the important features of **2c**, together with the atomic numbering scheme. It is clear that the geometry of the ligand **1b** has been significantly altered upon coordination. The structure of **2c** is comprised of discrete monomeric Pd(PhSeN(4-CH₃C₆H₄)CN-NC(4-CH₃C₆H₄)NSePh)(PPh₃) molecules in which the ligand is attached to palladium via N(1), N(3), and Se(1) in a tridentate fashion, forming two approximately planar five-membered rings. The geometry of the metal center is square planar, suggesting a formal divalent oxidation state for palladium. The Pd–P, Pd–N, and Pd–Se distances fall within the expected ranges¹⁷ and the complex is isostructural with its sulfur analogue **2a**. The details of the X-ray structural determinations of **2a** and **2b** were reported in the preliminary communication⁴ and will not be repeated here. However, selected bond distances and bond angles for **2a** and **2b** are summarized in Tables 4 and 5, respectively, for comparison with the corresponding parameters for **2c** and **2d**.

In addition to the remarkable conformational change, it is clear that the ligand contains an azine rather than a diazene moiety, i.e. the N(2)–N(3) distance of 1.414(7) Å is characteristic of an N–N single bond.¹⁸ This can be compared to the N(2)–

- (15) Pregosin, P.; Kunz, R. W. *³¹P and ¹³C NMR of Transition Metal Phosphine Complexes*, Diehl, P., Fluck, E., Kosfeld, R., Eds.; NMR Basic Principles and Progress 16; Springer-Verlag: New York, 1979.
- (16) (a) Edelmann, F.; Roesky, H. W.; Spang, C.; Noltemeyer, M.; Sheldrick, G. M. *Angew. Chem. Int. Ed. Engl.* **1986**, *25*, 931. (b) Kelly, P. F.; Woollins, J. D. *Polyhedron* **1989**, *8*, 290.
- (17) (a) Hursthouse, M. B.; Motevalli, M.; Kelly, P. F.; Woollins, J. D. *Polyhedron* **1989**, *8*, 997. (b) Allen, F. H.; Kennard, O.; Taylor, R. *Acc. Chem. Res.* **1983**, *16*, 146.
- (18) (a) Jones, R.; Kelly, P. F.; Williams, D. J.; Woollins, J. D. *J. Chem. Soc., Dalton Trans.* **1988**, 803. (b) Kumar Pal, C.; Chattopadhyay, S.; Sinha, C.; Chakravorty, A. *J. Organomet. Chem.* **1992**, *439*, 389. (c) Orpen, A. G.; Braumner, L.; Allen, F. H.; Kennard, D.; Watson, D. G.; Taylor, R. *J. Chem. Soc., Dalton Trans.* **1989**, S1.

Table 4. Selected Bond Distances (Å) for $M\{\text{PhENC}(4\text{-CH}_3\text{C}_6\text{H}_4)\text{N-NC}(4\text{-CH}_3\text{C}_6\text{H}_4)\text{NPh}\}\text{PPh}_3$ ($M = \text{Pd, Pt; E = S, Se}$)

	2a ^a	2b ^b	2c ^c	2d ^d
M(1)–P(1)	2.308(3)	2.279(3)	2.301(2)	2.272(4)
M(1)–N(1)	2.031(7)	2.031(8)	2.024(6)	2.02(1)
M(1)–N(3)	1.975(7)	1.987(7)	2.002(5)	1.98(1)
M(1)–E(1)	2.277(3)	2.266(3)	2.375(1)	2.368(2)
N(1)–C(7)	1.42(1)	1.41(1)	1.395(8)	1.40(1)
C(7)–N(2)	1.28(1)	1.26(1)	1.29(1)	1.26(1)
N(2)–N(3)	1.39(1)	1.41(1)	1.414(7)	1.41(1)
N(3)–C(15)	1.36(1)	1.34(1)	1.332(8)	1.35(1)
C(15)–N(4)	1.33(1)	1.31(1)	1.325(8)	1.33(1)
N(4)–E(1)	1.684(8)	1.725(8)	1.869(6)	1.89(1)
N(1)–E(2)	1.680(7)	1.682(8)	1.828(6)	1.83(1)

^a $M = \text{Pd, E = S}$. ^b $M = \text{Pt, E = S}$. ^c $M = \text{Pd, E = Se}$. ^d $M = \text{Pt, E = Se}$.

Table 5. Selected Bond Angles (deg) for $M\{\text{PhENC}(4\text{-CH}_3\text{C}_6\text{H}_4)\text{N-NC}(4\text{-CH}_3\text{C}_6\text{H}_4)\text{NPh}\}\text{PPh}_3$ ($M = \text{Pd, Pt; E = S, Se}$)

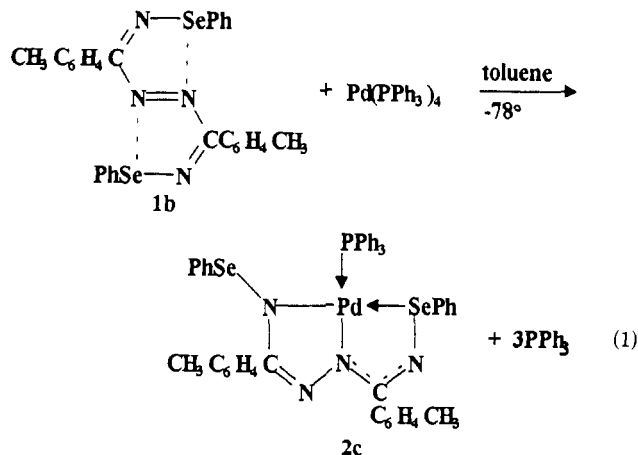
	2a ^a	2b ^b	2c ^c	2d ^d
P(1)–M(1)–N(1)	98.7(2)	99.9(2)	100.0(2)	100.0(3)
N(1)–M(1)–N(3)	78.7(3)	78.5(3)	79.1(2)	78.7(4)
N(3)–M(1)–E(1)	81.1(2)	81.6(2)	82.0(2)	82.3(3)
E(1)–M(1)–P(1)	101.53(10)	99.69(9)	98.56(7)	98.6(1)
M(1)–N(1)–C(7)	109.6(6)	110.0(6)	110.9(5)	110.3(9)
N(1)–C(7)–N(2)	122.0(8)	122.8(9)	121.9(8)	122(1)
C(7)–N(2)–N(3)	111.3(8)	111.6(8)	112.0(6)	111(1)
N(2)–N(3)–M(1)	118.0(6)	117.0(5)	115.8(4)	116.6(7)
M(1)–N(3)–C(15)	120.6(6)	119.8(6)	122.4(5)	122.8(9)
N(3)–C(15)–N(4)	120.7(8)	122.9(9)	124.2(7)	124(1)
C(15)–N(4)–E(1)	115.2(6)	114.1(7)	113.3(5)	112.4(9)
N(4)–E(1)–M(1)	101.8(3)	101.3(3)	97.6(2)	97.9(3)

^a $M = \text{Pd, E = S}$. ^b $M = \text{Pt, E = S}$. ^c $M = \text{Pd, E = Se}$. ^d $M = \text{Pt, E = Se}$.

N(3) bond distance of 1.39(1) Å in **2a** and the N=N distance of 1.263(4) Å in **1c**.^{3b} Furthermore, the C(7)–N(2) bond distance of 1.29(1) Å in **2c** also demonstrates the presence of a C=N double bond (cf. the corresponding C–N distances of 1.433(5) Å in **1c**^{3b} and 1.28(1) Å in **2a**⁴). The N(3)–C(15) and C(15)–N(4) bond distances of 1.332(8) and 1.325(8) Å, respectively, are almost identical and indicate an even more extensive delocalization in the NCN segment of the second five-membered ring than observed in the analogous Pd–S complex **2a**. The Se(1)–N(4) bond length of 1.869(6) Å is slightly longer than the Se(2)–N(1) distance of 1.828(6) Å, a consequence of the coordination of Se(1) to Pd (cf. Se–N distances of ca. 1.817(3) Å in **1c**^{3b}). Interestingly, the corresponding S–N bond lengths in **2a** are almost identical (see Table 4).

Hence, the reaction of the selenium-substituted diazene **1b** with $\text{Pd}(\text{PPh}_3)_4$, like that of the corresponding sulfur system, results in the formation of a metallacycle via an internal redox process, i.e. the formal reduction of the diazene N=N double bond and subsequent formation of a palladium(II) azine species (eq 1). A rare related example is the reaction of $\text{Cp}_2\text{Ti}(\text{CO})_2$ with $\text{RO}_2\text{CN}=\text{NCO}_2\text{R}$, which produces $\text{Cp}_2\text{Ti}(\text{RO}_2\text{CN}=\text{NCO}_2\text{R})$ in which the ligand is thought to be coordinated in a bidentate (O, N) fashion to Ti.¹⁹ A structural determination was not reported.

The lack of observation of $^2J(^{31}\text{P}-^{77}\text{Se})$ for **2c** and **2d** (*vide infra*) is puzzling since typical literature values for *cis*- $^{31}\text{P}-^{77}\text{Se}$ couplings in metal complexes are in the range 25–30 Hz.²⁰ Consequently, we cannot rule out the possibility that Pd–Se (or Pt–Se, in the case of **2d**) dissociation occurs in solution.



Reaction of **1b with $(\text{C}_2\text{H}_4)\text{Pt}(\text{PPh}_3)_2$.** The reaction of equimolar amounts of **1a** or **1b** with $(\text{C}_2\text{H}_4)\text{Pt}(\text{PPh}_3)_4$ in toluene at -78°C results in the isolation of **2b** and **2d** in 65% and 42% yields, respectively. Both **2b** and **2d** were obtained as air-stable yellow crystals. The $^{31}\text{P}\{\text{H}\}$ NMR spectra of THF solutions of **2b** or **2d** show a singlet at ca. 19 ppm with $^1J(^{195}\text{Pt}-^{31}\text{P})$ values of 3610–3630 Hz, while the ^1H NMR spectra indicate the presence of two inequivalent 4- $\text{CH}_3\text{C}_6\text{H}_4$ groups. $^2J(^{31}\text{P}-^{77}\text{Se})$ coupling was not observed. Unfortunately, the instability of **2d** in solution at ambient temperatures precludes the measurement of a ^{77}Se NMR spectrum. The spectroscopic results suggest that the structure of **2d** is similar to that of the corresponding Pt–S system (**2b**) and this was confirmed by an X-ray crystallographic study of **2d** (see below).

Monitoring of the crude reaction mixture by ^{31}P NMR spectroscopy reveals that the reaction of **1b** with $(\text{C}_2\text{H}_4)\text{Pt}(\text{PPh}_3)_2$ does not proceed cleanly. In addition to the resonances observed for **2d** and free PPh_3 , a third signal at ca. 27 ppm is observed which does not show ^{195}Pt satellites (cf. Ph_3PSe , $\delta(^{31}\text{P}) = 35.8$ ppm²¹). Preliminary thermolysis experiments indicate that this signal appears as a result of decomposition of **2d**, which is quite thermally unstable in solution. However, attempts to isolate this product or a Pt-containing species have been unsuccessful. In comparison, the metal–sulfur complexes **2a** and **2b** are stable in solution.

Crystal and Molecular Structure of **2d.** An ORTEP plot illustrating the important features of **2d** is shown in Figure 2. The structure is comprised of discrete monomeric $\text{Pt}(\text{PhSeN}(4\text{-CH}_3\text{C}_6\text{H}_4)\text{CN-NC}(4\text{-CH}_3\text{C}_6\text{H}_4)\text{NSePh})(\text{PPh}_3)$ molecules in which the ligand is attached to platinum via N(1), N(3), and Se(1) in a tridentate fashion, forming two approximately planar five-membered rings. There are no significant differences in either geometry or configuration between **2b** and **2d** (see Tables 4 and 5, and the two structures are isomorphous). All bond distances and bond angles involving platinum lie within the expected ranges.²³ The N–N bond distances in the ligands are 1.41(1) and 1.40(1) Å for **2b** and **2d**, respectively. Thus the reactions of **1a** and **1b** with $\text{Pt}(\text{C}_2\text{H}_4)(\text{PPh}_3)_2$ can be viewed as an oxidative addition with formal reduction of the $-\text{N}=\text{N}-$ group of the ligand to an azine.

FAB Mass Spectrometric Studies. FAB mass spectra were obtained for the metallacycles **2a–d** using a nitrobenzyl alcohol/ CH_2Cl_2 matrix. Selected m/z data are presented in Table 6. The molecular ion cluster was observed as the major peak for both metal–sulfur complexes **2a** and **2b**. The predominant ion observed

(19) (a) Einstein, F. W. B.; Sutton, D.; Tyers, K. G. *Inorg. Chem.* **1987**, *26*, 111. (b) Perera, S. D.; Shaw, B. L.; Thornton-Pett, M. *J. Chem. Soc., Dalton Trans.* **1992**, 1469.
(20) (a) Jewiss, H. C.; Levason, W.; Spicer, M. D.; Webster, M. *Inorg. Chem.* **1987**, *26*, 2102. (b) Harbron, S. K.; Higgins, S. J.; Hope, E. G.; Kemmitt, T.; Levason, W. *Inorg. Chim. Acta* **1987**, *130*, 43.

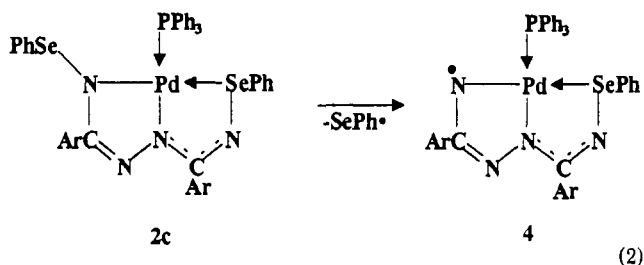
(21) Avar, G.; Russler, W.; Kisch, H. Z. *Naturforsch.* **1987**, *42b*, 1441.
(22) Burford, N.; Royan, B. W.; Spence, R. E. v. H.; Rogers, R. D. *J. Chem. Soc., Dalton Trans.* **1990**, 2111.
(23) (a) Chivers, T.; Edwards, M.; Kapoor, P. N.; Meetsma, A.; van de Grampel, J. C.; van der Lee, A. *Inorg. Chem.* **1990**, *29*, 3068. (b) Chattopadhyay, S.; Sinha, C.; Basu, P.; Chakravorty, A. *J. Organomet. Chem.* **1991**, *414*, 429.

Table 6. FAB Mass Spectrometric Data for $M\{\text{PhEN}(4\text{-CH}_3\text{C}_6\text{H}_4)\text{CN-NC}(4\text{-CH}_3\text{C}_6\text{H}_4)\text{NEPh}\}\text{PPh}_3$ (**2**)

	<i>m/z</i>	identity	intens
2a	848	M^+	100
	740	$[(M + H) - \text{SPh}]^+$	38
2b	938	$[M + H]^+$	100
	831	$[(M + H) - \text{SPh}]^+$	17
2c	788	$[(M + H) - \text{SePh}]^+$	100
2d	1033	$[(M + H)]^+$	20
	877	$[(M + H) - \text{SePh}]^+$	18

in the molecular ion region for **2a** corresponds to M^+ rather than the protonated $[M + H]^+$. The protonated molecular ion is still observed but its intensity is lower than that of the molecular ion. A number of recent studies have reported compounds which do not generate $[M + H]^+$ as the predominant ions under FAB conditions.²⁴ The reasons for this are still not well understood.

The next major peaks observed in the spectra of **2a** and **2b** correspond to fragments formed by the cleavage of an N-S bond, i.e. loss of an SPh moiety. Interestingly, the FAB mass spectrum of the metal-selenium complex **2c** does not show a molecular ion cluster. Instead the major peak observed corresponds to an $[(M + H) - \text{SePh}]^+$ ion, which suggests that an Se-N bond in this complex is readily cleaved. Although we have no direct evidence, it is reasonable to propose that the bond cleaved involves the Se atom which is not coordinated to the metal (eq 2). A molecular ion cluster of low intensity is observed for **2d**.



Electrochemical Studies. Compounds **2a** and **2b** both undergo reversible one-electron oxidations at +0.62 and +0.66 V vs SCE, respectively. In both cases the peak to peak separations of the waves are Nernstian, and it is believed that the oxidations are ligand-based in origin. A possible oxidation site within the ligand is at the uncoordinated sulfur atom. The species formed from the oxidation of **2a** is quite unstable; the electrochemical response only becomes reversible at scan rates of $>800 \text{ mV}^{-1} \text{ s}$. For **2b**, the stability of the oxidized species is in the region of several

seconds. Spectroelectrochemical experiments were performed in an effort to further characterize the oxidized species, however isobestic points could not be detected in the UV-visible spectra.

Neither compound exhibits a reduction response in the range 0 to -1.8 V vs SCE. For comparison, the diazene *trans*- $[\text{PhSeN}(\text{Ph})\text{CN}=\text{NC}(\text{Ph})\text{NSePh}]$ undergoes a reversible one-electron reduction in acetonitrile at -0.51 V vs SCE, producing the corresponding anion radical.^{3b} An oxidation response is not observed.

Reactions of 1a with Nickel(0) Complexes. Since it is known that azobenzene forms η^2 -bonded complexes with Ni^0 [e.g. $\{(4\text{-CH}_3\text{C}_6\text{H}_4)\text{P}_3\}_2\text{Ni}(\text{N}_2\text{Ph}_2)$ ²⁵ and $(t\text{-BuNC})_2\text{Ni}(\text{N}_2\text{Ph}_2)$ ²⁶], it was of interest to explore the coordination chemistry of **1a** with Ni^0 . A solution of $(\text{PhCH}=\text{CHPh})\text{Ni}(\text{PMe}_2\text{Ph})_2$ ²⁷ in toluene ($\delta(^{31}\text{P}) = -1.5 \text{ ppm}$) was treated with an equimolar amount of **1a** to give a dark brown solution which exhibited a singlet at 39.92 ppm, in addition to several minor resonances at lower frequency. However, all attempts to isolate a pure product were unsuccessful.

Conclusions. The reaction of both the sulfur- and selenium-substituted diazenes **1a** and **1b** with zerovalent Pt and Pd produces the isostructural azine metallacycles $M(\text{PhEN}(4\text{-CH}_3\text{C}_6\text{H}_4)\text{CN-NC}(4\text{-CH}_3\text{C}_6\text{H}_4)\text{NEPh})(\text{PPh}_3)$ ($M = \text{Pd}, \text{Pt}; E = \text{S}, \text{Se}$). The formation of the metallacycles occurs via an internal redox reaction, resulting in the reduction of the diazene N=N double bond and the subsequent formation of a formally divalent metal complex. This is an unexpected result, since previous studies of the coordination chemistry of diazenes and chalcogen-nitrogen compounds suggest that coordination of **1a** and **1b** might occur via the nitrogen and/or chalcogen atoms, η^2 -complexation of the N=N moiety, or even insertion of the metal into an N-E bond. The selenium derivatives **2c** and **2d** were found to be thermally less stable than their corresponding sulfur analogues **2a** and **2b**. FAB mass spectroscopic studies of the metallacycles **2** demonstrate that cleavage of an N-E bond may be readily achieved, particularly for $\text{Pd}(\text{PhSeN}(4\text{-CH}_3\text{C}_6\text{H}_4)\text{CN-NC}(4\text{-CH}_3\text{C}_6\text{H}_4)\text{NSePh})(\text{PPh}_3)$ (**2c**).

Acknowledgment. We thank Dr. R. Yamdagni and Mrs. D. Fox for obtaining the FAB mass spectra and Dr. A. S. Hinman and Mr. P. Wiebe for their assistance with the electrochemical experiments. The financial support of the NSERC (Canada) in the form of an operating grant (T.C.) and an International Fellowship (K.M.) is gratefully acknowledged.

Supplementary Material Available: Tables listing crystallographic experimental details, bond distances and bond angles, torsion angles, and anisotropic temperature factors for **2c** and **2d** (24 pages). Ordering information is given on any current masthead page.

(25) Ittel, S.; Ibers, J. A. *J. Organomet. Chem.* **1973**, *57*, 389.

(26) Dickson, R. S.; Ibers, J. A. *J. Am. Chem. Soc.* **1972**, *94*, 2988.

(27) Sillet, G.; Ricard, L.; Patois, C.; Mathey, F. *J. Am. Chem. Soc.* **1992**, *114*, 9453.

(24) Bruce, M. I.; Liddell, M. J. *J. Appl. Organomet. Chem.* **1987**, *1*, 191.